Imaging androgen receptor function during flutamide treatment in the LAPC9 xenograft model

Romyla Ilagan,[1] Liquin Joann Zhang,[1] Jill Pottratz,[1] Kim Le,[1] Sussan Salas,[1] Meera Iyer,[3] Lily Wu,[2,3] Sanjiv S. Gambhir,[3] and Michael Carey[1]

Departments of [1]Biological Chemistry, [2]Urology, and [3]Molecular and Medical Pharmacology, School of Medicine, University of California at Los Angeles, Los Angeles, California

Abstract

The current understanding of the response of androgen receptor to pharmacologic inhibitors in prostate cancer is derived primarily from serum prostate-specific antigen (PSA) levels. In this study, we test whether a novel androgen receptor–specific molecular imaging system is able to detect the action of the antiandrogen flutamide on androgen receptor function in xenograft models of prostate cancer. Adenoviruses bearing an optical imaging cassette containing an androgen receptor–responsive two-step transcriptional amplification system were injected into androgen-dependent and hormone-refractory tumors of animals undergoing systemic time-controlled release of the antiandrogen flutamide. Imaging of tumors with a cooled charge-coupled device camera revealed that the response of AdTSTA to flutamide is more sensitive and robust than serum PSA measurements. Flutamide inhibits the androgen signaling pathway in androgen-dependent but not refractory tumors. Analysis of androgen receptor and RNA polymerase II binding to the endogenous *PSA* gene by chromatin immunoprecipitation revealed that flutamide treatment and androgen withdrawal have different molecular mechanisms. The application of imaging technology to study animal models of cancer provides mechanistic insight into antiandrogen targeting of androgen receptor during disease progression. [Mol Cancer Ther 2005;4(11):1662–9]

Introduction

Prostate cancer is a disease driven by the androgen receptor (1–4). Androgen receptor is a 110-kDa steroid receptor, which is sequestered in the cytoplasm by chaperones in the absence of its ligand. In the presence of dihydrotestosterone, androgen receptor dimerizes and enters the nucleus, where it binds to androgen response elements and activates transcription of responsive genes. One of the key challenges in prostate cancer research has been determining how androgen receptor functions in recurrent or androgen-independent prostate cancer (also called hormone-refractory prostate cancer; refs. 5–11) and how pharmacologic inhibitors affect function (12). Our groups have been addressing this problem using gene expression–based bioluminescence imaging to evaluate androgen receptor function in xenograft models (13–16), which accurately recreate prostate cancer progression from an androgen-dependent to an androgen-independent phase (17).

Imaging provides a means to probe the mechanism of cancer in live animals and facilitates the evaluation of pharmacologic effects on specific signaling events. In this study, we address the mechanism of a nonsteroidal antiandrogen called flutamide by molecular imaging of androgen receptor function and compare the results with the effects of androgen deprivation by castration. Flutamide is more potent than Casodex in mice (18, 19). We chose this drug to address whether a specialized molecular imaging system could be employed to detect the inhibitory effect of an antiandrogen on androgen receptor function during prostate cancer growth.

In gene expression–based bioluminescence imaging, a promoter is placed upstream of a bioluminescence reporter gene (20–22). The reporter cassette is introduced into tumor cells in an animal and the promoter activity is imaged after injection of D-luciferin (for firefly luciferase) or coelenterazine (for *Renilla* luciferase) using a Xenogen *in vivo* imaging system (Xenogen Corp., Alameda, CA; ref. 23). *In vivo* imaging system is a cooled charge-coupled device that measures bioluminescent light. A computer interprets the light and superimposes a pseudoimage, representing the quantity of photons emitted by the tissue, over a gray-scale photograph of the animal.

A major challenge in bioluminescence imaging is that cellular promoters are typically weak, and detection of optical signals in dense tissues is hampered by light attenuation and scattering (20, 24). We developed an approach to augment cellular promoter activity and light output based on a concept termed two-step transcriptional amplification (TSTA; ref. 16). A cellular promoter expresses a potent chimeric activator, GAL4-VP16. GAL4-VP16 is a fusion of the high-affinity yeast GAL4 DNA-binding domain to the potent herpes simplex virus VP16 activation domain (25, 26). GAL4-VP16 has a unique potency and specificity not naturally found in mammalian cells. GAL4-VP16 binds a GAL4-responsive reporter gene and generates high levels of firefly luciferase. Our prostate cancer–specific

Received 6/15/05; revised 8/8/05; accepted 8/30/05.

The costs of publication of this article were defrayed in part by the payment of page charges. This article must therefore be hereby marked advertisement in accordance with 18 U.S.C. Section 1734 solely to indicate this fact.

Note: S.S. Gambhir is currently at the Molecular Imaging Program at Stanford, Stanford University School of Medicine, James H. Clark Center, E13 318 Campus Drive, Stanford, CA 94305-5472.

Requests for reprints: Romyla Ilagan, Department of Biological Chemistry, School of Medicine, University of California at Los Angeles, 10833 Le Conte Avenue, CHS 33-142, Los Angeles, CA 90095-1737. Phone: 310-794-9636; Fax: 310-206-5272. E-mail: milagan@ucla.edu

doi:10.1158/1535-7163.MCT-05-0197

version of the TSTA system employs a modified prostate-specific antigen (PSA) promoter, which responds more robustly than the native promoter to the androgen receptor (27). It also contains a more potent derivative of GAL4-VP16, where the VP16 activation domain is dimerized (GAL4-VP2; ref. 22).

We employed this optimized androgen receptor–responsive TSTA vector to generate adenovirus (AdTSTA) and lentivirus (13, 14, 28, 29), where we could sensitively measure androgen receptor signaling in xenograft tumors or native prostate tissue within live animals. An advantage of the AdTSTA approach is the ability to inject the virus into any tumor in any xenograft animal. Many of the xenografts do not exist as cell lines, placing a limitation on the development of stably transformed cells. We therefore used the adenovirus to image existing human xenografts in severe combined immunodeficient mice, and our results have addressed several questions about androgen receptor function in recurrent cancer.

Imaging of AdTSTA in LAPC9 xenografts, which express wild-type androgen receptor and PSA, revealed the loss of androgen receptor activity on androgen withdrawal by castration and the resuscitation of activity as the tumor transitioned into the recurrent state (14). Numerous biological benchmarks of androgen receptor function correlated closely with the imaging measurements. In androgen-dependent tumors, the serum PSA levels increased with tumor size, androgen receptor bound to the endogenous PSA promoter and enhancer, and RNA polymerase II was bound both at the promoter and in the act of transcribing downstream exons. Androgen withdrawal by castration led to decreased serum PSA levels, decreased androgen receptor levels, and cytoplasmic localization of androgen receptor in the xenograft tumors. Furthermore, chromatin immunoprecipitation analysis revealed a loss of androgen receptor from the PSA promoter and enhancer. Surprisingly, on castration, polymerase II remained bound at the promoter, although androgen receptor binding was substantially reduced. On transition of the tumor into the androgen-independent stage, the androgen receptor levels increased, androgen receptor relocalized to the nucleus and bound to the PSA enhancer and promoter, and polymerase II bound at both the promoter and the downstream exons. The data collectively argued that androgen receptor is fully active in androgen-independent cancer.

Much has been learned about androgen receptor response to antiandrogens in cell lines, but little is known of how antiandrogen treatment affects androgen receptor activity in androgen-dependent and recurrent tumors in animal models and how the effects compare to androgen withdrawal. In this study, we tested the effect of a nonsteroidal antiandrogen called flutamide used clinically to treat prostate cancer. Our study was designed to address three key questions: (*a*) Can androgen receptor–specific, gene expression–based imaging measure the response to the antiandrogen flutamide in a living subject? (*b*) Is imaging more sensitive than conventional benchmarks, such as serum PSA levels or tumor size? and (*c*) Does inhibition of the androgen signaling pathway by flutamide employ a similar mechanism as androgen deprivation in the context of the tumor?

We found that AdTSTA was more sensitive than serum PSA in measuring the inhibitory effect of flutamide. The imaging measurements allowed us to identify time points at which to analyze changes in androgen receptor within the tumor environment that accompany the onset of the therapeutic effect. These alterations suggest fundamental differences between androgen withdrawal and antiandrogen treatment, which may be related to the mechanism of hormone resistance.

Materials and Methods

Animal Charge-Coupled Device Experiments

The imaging was done essentially as we described previously (13). Animal care and euthanasia were done with the approval of the University of California at Los Angeles Animal Research Committee. The mice were first anesthetized with ketamine-xylazine mix (4:1). Imaging was done using a Xenogen *in vivo* imaging system 100 cooled charge-coupled device camera. The mice were injected with 200 μL of 15 mg/mL D-luciferin i.p. 15 minutes before imaging, after which they were placed in a light-tight chamber. A gray-scale reference image was obtained followed by the acquisition of a bioluminescent image. The acquisition time ranged from 1 to 2 minutes. The images shown are pseudoimages of the emitted light in photons/s/cm^2/steradian superimposed over the gray-scale photographs of the animal. We used LAPC9 animals bearing tumors of 0.4 cm in diameter to study the flutamide response as larger tumors were relatively unresponsive. Briefly, on day 1, 10^7 plaque-forming units of AdTSTA were injected in two locations. Imaging generally commenced 3 days later. On day 3, flutamide (25 mg/60-day release) or placebo pellets (Innovative Research, Sarasota, FL) were implanted s.c. on the dorsal side of the mouse. Time courses were done where mice were imaged every 3 to 4 days. Because adenoviral injection delivers slightly different amounts of vector to the tumors due to viral leakage, we obtained a baseline image 3 days after viral injection and measured the percent change in signal over time. The data were analyzed statistically using Student's *t* test as described previously (14).

Immunoblots

Whole tumors were harvested from mice via surgical removal at the imaging end points and immediately frozen in liquid N_2. Frozen tumors were homogenized using a mortar and pestle in the presence of liquid N_2. Samples were then resuspended in 400 to 600 μL radioimmunoprecipitation assay buffer (10 mmo/L Tris-HCl, 1% NP40, 1% sodium deoxycholate, 150 mmo/L NaCl, 1 mmo/L EDTA, 0.2% SDS, 1 mmo/L phenylmethylsulfonyl fluoride, 1 μg/mL leupeptin and pepstatin, 1 mmo/L Na_3VO_4, 1 mmo/L NaF). Lysates were passed through 25-gauge needles to shear genomic DNA followed by

centrifugation at 14,000 × *g* at 4°C for 20 minutes. Samples were assayed for total protein concentration using the Pierce (Rockford, IL) BCA Protein Assay kit and further normalized using γ-tubulin or cytokeratin-8 antibodies for loading controls. Extracts were fractionated on 4% to 15% Tris-HCl Ready Gels and immunoblotted. Antibodies against androgen receptor M-441 (sc-7305), γ-tubulin (D-10; sc-17788), and cytokeratin-8 (sc-802) were obtained from Santa Cruz Biotechnology (Santa Cruz, CA). Antibodies to transcription factor IIB were generated in our laboratory.

Chromatin Immunoprecipitation

Chromatin immunoprecipitation was done on formaldehyde cross-linked tumor samples essentially as described using antibodies to androgen receptor and polymerase II (14).

Results

Imaging Provides a Sensitive Indicator of Androgen Receptor Inhibition

Figure 1A illustrates the androgen receptor–responsive, gene expression–based imaging cassette inserted within AdTSTA and used in the experiments described below (14). The system sensitively measures androgen receptor activity in prostate tissues by expressing firefly luciferase, which is detected using a Xenogen *in vivo* imaging system. Our previous studies have shown that the amount of firefly luciferase activity is proportional to the activity of androgen receptor both *in vitro* and in animals (13, 14). Further, the AdTSTA approach was highly successful in quantifying the loss of tumor androgen receptor function by castration and the resuscitation of activity as the tumor transitioned to a recurrent phase. Based on these results, we surmised that the system would be able to detect the effect of small-molecule inhibitors directed at androgen receptor.

One of the strengths of the AdTSTA imaging system is the ability to noninvasively and repetitively monitor individual animals to compare the signaling pathway with clinical measurements of tumor function. Figure 1 shows the results of a typical experiment, where two intact male severe combined immunodeficient mice bearing LAPC9 tumors were injected with AdTSTA (day 1) after the tumors had reached ~0.4 cm average diameter by caliper measurement. After taking a baseline charge-coupled device measurement on day 3 following injection of AdTSTA, the two mice were implanted with either a

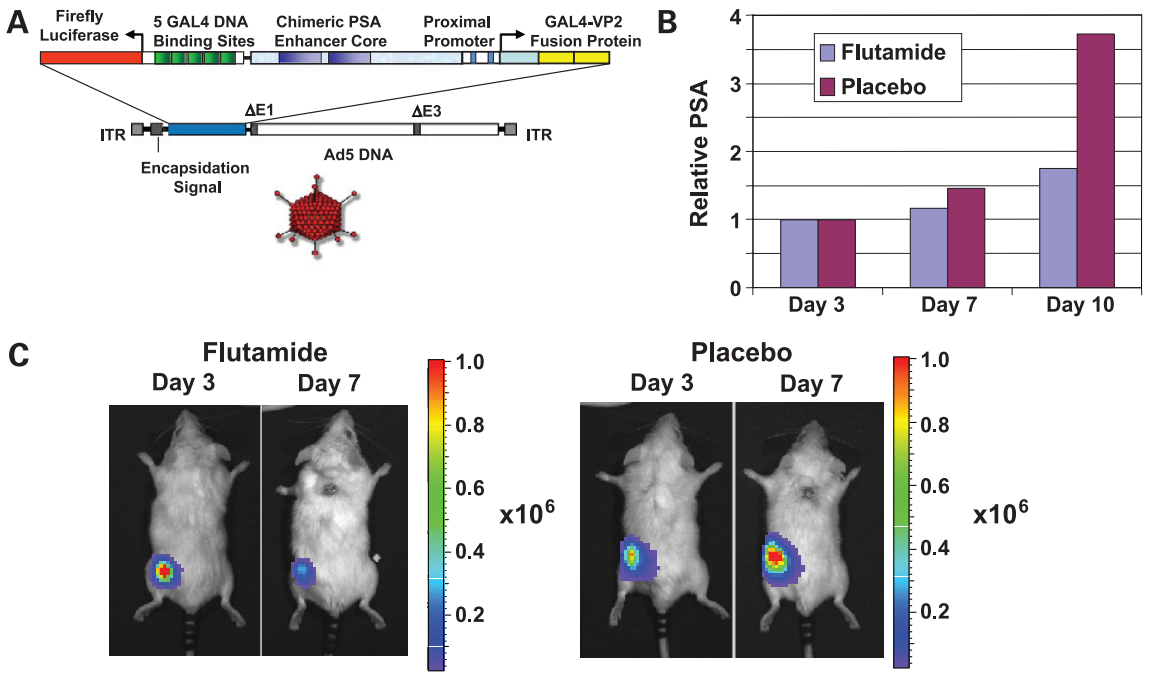

Figure 1. AdTSTA detects response of androgen-dependent tumors to flutamide. **A,** AdTSTA cassette. AdTSTA contains two copies of the PSA enhancer placed upstream of the natural promoter (13, 27). Immediately downstream of the start site is a gene encoding GAL4-VP2, a fusion of amino acids 1 to 147 of GAL4, containing the GAL4 DNA-binding domain, fused to two copies of the herpes simplex virus VP16 activation domain (amino acids 413-454; ref. 26). A GAL4-responsive reporter gene is positioned upstream of the PSA enhancers but in the opposite direction. The reporter contains five GAL4 sites upstream of the adenovirus E4 promoter driving firefly luciferase. **B,** serum PSA levels. Serum was taken from the mice by orbital bleed and subjected to serum PSA measurements using the American Qualex (San Clemente, CA) PSA ELISA kit (KD4310). The two levels were normalized to 1, and the fold change over time was monitored on days 7 and 10 postinjection. *Columns,* average of triplicate serum PSA measurements ($n = 6$; $P = 0.049$). **C,** inhibition by flutamide in typical animals. LAPC9 tumors were grown to 0.4 cm in severe combined immunodeficient mice and injected on day 0 with AdTSTA. On day 3 postinjection of AdTSTA, a baseline image was taken using a Xenogen *in vivo* imaging system charge-coupled device camera and the mice were implanted with placebo or flutamide slow-release pellets (25 mg/60-day release). The mice were imaged on day 7 to monitor the short-term effects of flutamide on the androgen receptor pathway. Typical images are shown. The firefly luciferase activity is measured in light units of photons/s/cm^2/steradian.

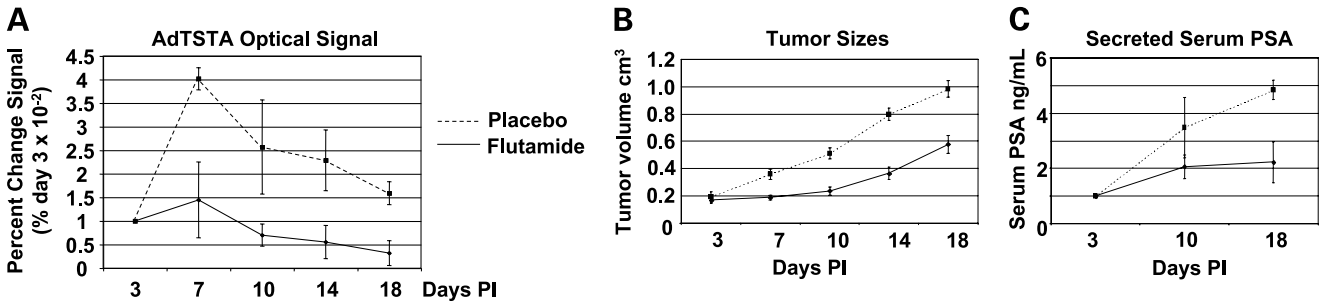

Figure 2. Comparison of imaging signals, PSA levels, and tumor volumes for cohorts. **A,** imaging of LAPC animals. Cohorts of nine flutamide-treated and six placebo-treated animals were subjected to imaging. The maximal imaging signals for the placebo and flutamide cohorts were averaged and plotted as the percent change versus the baseline image taken on day 3 postinjection (*PI*) of AdTSTA. **B,** tumor volumes were estimated based on the average diameter using calipers. Measurements were taken at the indicated time points. The percent changes versus the values measured on day 3 were measured and averaged. *Points,* mean; *bars,* SD. Student's *t* test was used to determine significance. **C,** PSA levels were measured by serum ELISA and measured in parallel to the imaging. Blood samples were taken by retro-orbital sinus bleed from alternating eyes according to the University of California at Los Angeles Animal Research Committee regulations. Values were averaged on day 3, and placebo- and flutamide-treated cohorts were separated and measured on days 10 and 18.

flutamide time-release pellet or a placebo pellet. We then monitored the change in signal over time versus the baseline measurement. In parallel, we measured the PSA levels of the animals to compare with the imaging measurements. Figure 1B shows that significant PSA differences between placebo-treated and flutamide-treated animals are only observed on day 10. However, the charge-coupled device images in Fig. 1C shows that on day 7 postinjection, when PSA levels have not changed significantly, the imaging detects an increase in androgen receptor signaling in the placebo-treated animal and a decrease in the flutamide-treated animal. We conclude that the TSTA system can detect the antiandrogenic effects of flutamide paralleling the clinical effects of the antiandrogen in man.

Pathway Inhibition Versus Tumor Growth and PSA

A key issue in understanding the action of pharmacologic inhibitors is whether the inhibitor reaches its site of action in living subjects and whether inhibition of the pathway truly inhibits tumor growth to the same extent. The experiment in Fig. 2 addresses this issue by comparing the flutamide responses of the AdTSTA imaging system, serum PSA levels, and tumor size over time. The three graphs illustrate the changes in average charge-coupled device signals (Fig. 2A), tumor sizes (Fig. 2B), and serum PSA levels (Fig. 2C) for the flutamide ($n = 9$) and placebo ($n = 6$) cohorts from 3 to 18 days after injection of the AdTSTA imaging vector. The imaging signal increases on day 7, 4 days after the placebo and flutamide pellets were implanted, and then begins to drop gradually over time. The increase in signal is expected as the virus begins to respond to the cellular environment and generates increased levels of luciferase. After steady-state levels are reached, the signals begin to diminish in LAPC9 androgen-dependent tumors. AdTSTA, unlike the tumor cells, does not replicate and the optical signal diminishes gradually as the tumor burden increases due to increased light absorption by the tissue. Despite this caveat, there is a significant and consistent difference averaging ~250% in the charge-coupled device signal between the placebo and the flutamide cohorts from day 7 ($P = 0.03$) to day 18 ($P = 0.004$).

The differences in PSA levels were noticeable on day 10, but the P was not significant ($P = 0.3$). As the tumors reached their maximal sizes on day 18 (Fig. 2B), the difference between treated and untreated cohorts became apparent but not statistically significant. This was not as accurate as the imaging values ($P = 0.004$). We conclude that imaging detects a significant reduction of androgen receptor signaling at time points where PSA levels are similar.

Androgen Receptor Levels and Chromatin Immunoprecipitation in Flutamide-Treated Tumors

To further understand the molecular consequences of flutamide action on androgen receptor, we employed the imaging analysis to identify time points when the effect of flutamide was evident (4 days after initiating treatment). At this stage, tumors were harvested and subjected to immunoblot and chromatin immunoprecipitation analyses to determine the levels of androgen receptor and its ability to bind the PSA enhancer.

Comparison of androgen receptor levels in tumors from animals castrated 4 days before harvest revealed that androgen receptor levels decrease significantly relative to several other gel loading controls, such as γ-tubulin and transcription factor IIB (Fig. 3A). We reported previously that this decrease was associated with reduced serum PSA levels and a reduced AdTSTA imaging signal. Additionally, chromatin immunoprecipitation analysis revealed a significant decrease in binding of androgen receptor to the PSA enhancer and promoter in castrated state and a increase in the androgen-independent state (14).

In contrast to the results in castrated animals, we observed a consistent 2-fold increase in androgen receptor levels 4 days after treatment in the flutamide-treated versus

placebo-treated animals as shown for two representative individuals each (Fig. 3B). The data suggest that flutamide stabilizes androgen receptor in the tumor, much like the effect of dihydrotestosterone (30, 31).

A key question was whether transcription complexes were forming on the *PSA* gene. Flutamide and a related inhibitor Casodex (bicalutamide), not used in this study, have been widely reported as facilitating the nuclear localization of androgen receptor, and previous reports have suggested that bicalutamide promotes binding of androgen receptor to the PSA regulatory region in LNCaP cell lines (32–34). Additionally, we reported previously that transcription factors, including polymerase II, remained bound to the promoter of the *PSA* gene under conditions where castration had led to decreased levels and binding of androgen receptor in LAPC9 tumors (14). We therefore probed the PSA enhancer in the LAPC9 tumors by chromatin immunoprecipitation to determine if the enhanced levels of androgen receptor reflect functional binding even while the *PSA* gene is relatively inactive. Figure 4B shows that androgen receptor is indeed bound to the PSA enhancer in the presence and absence of flutamide (compare *lanes 1* and *2*). Although androgen receptor is bound in androgen-independent tumors, it is bound less well consistent with the decreased androgen receptor levels typically found in our xenograft model.

Although androgen receptor is bound to the promoter, the imaging and PSA data suggest that the gene is largely inactive. To confirm that transcription was indeed inactivated, we probed the promoter for the presence of RNA polymerase II (Fig. 4C). Although polymerase II is bound to the PSA promoter in androgen-dependent, androgen-independent, and castrated tumors, it nearly disappears from the promoter in the presence of flutamide despite the presence of androgen receptor at the enhancer. The data illustrate that in the context of the tumor the effects of androgen withdrawal by castration and the antiandrogenic effects of flutamide are fundamentally different.

Flutamide Insensitivity in Androgen-Independent Cancer

The inability of the antiandrogens flutamide and Casodex to inhibit androgen receptor in androgen-independent cancer is one of the reasons men eventually die from metastatic disease (35). Although these drugs elicit transient effects in patients, the androgen insensitivity of the tumor prevents the drugs from functioning. Indeed, in some individuals, flutamide and Casodex begin to act as agonists (36–38).

Figure 5 compares the effect of placebo and flutamide treatment on androgen receptor activity in androgen-dependent and androgen-independent LAPC9 tumors. Whereas the androgen-dependent tumors are grown in intact male mice, the androgen-independent tumors are stably propagated in castrated male severe combined immunodeficient mice. Figure 5A shows that in typical animals, by day 18, the imaging signal in androgen-dependent tumors has decreased below the baseline observed on day 3 (compare the animals in Fig. 5A, *top*). In contrast, we observe no inhibition of androgen receptor function in androgen-independent tumors over the same period.

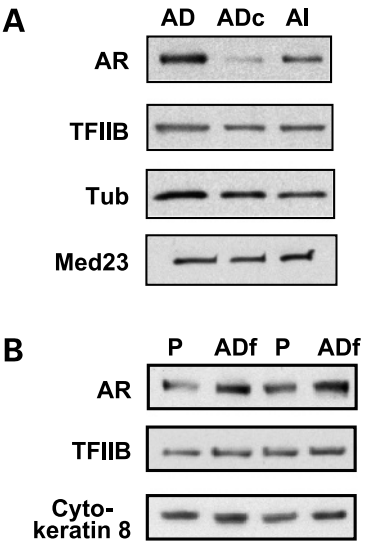

Figure 3. Androgen receptor levels in treated tumors. Whole-cell tumor extracts were prepared by freezing tumors in liquid N_2 followed by crushing with a mortar and pestle. The crushed tissue was resuspended in radioimmunoprecipitation assay buffer, heated, and fractionated on SDS polyacrylamide gels. The extracts were blotted onto nitrocellulose and normalized to γ-tubulin (*Tub*) or cytokeratin-8. **A,** comparison of androgen-dependent, castrated, and androgen-independent tumors. *AD,* extract from tumors grown in intact male mice; *ADc,* samples from androgen-dependent tumors after castration (castration was done 4 d before harvest of the tumor); *AI,* tumors grown in castrated mice. **B,** effects of flutamide. *P* and *ADf,* tumors treated with placebo or flutamide, respectively, for 4 d. The blots were developed by chemiluminescence. Representative data are shown. Fold differences were determined using Molecular Dynamics (Sunnyvale, CA) laser densitometer using ImageQuant 5.2 software.

These observations are reflected in the graph, which plots the change in signal from days 3 to 18 in placebo- and flutamide-treated cohorts (Fig. 5B). In placebo-treated animals, the optical signals were higher relative to flutamide-treated tumors by day 18 consistent with the previous experiment ($P = 0.045$; see Fig. 2). In contrast, the signals in the flutamide-treated androgen-independent animals were similar to the placebo cohort.

Discussion

The use of bioluminescence imaging in combination with molecular analysis is an emerging paradigm for tumor studies in preclinical models of cancer. An important application of imaging is to determine whether a drug is reaching its intended target within a living subject and to determine whether the efficacy of target inhibition correlates with the therapeutic effect. This latter issue represents a key challenge in the pharmaceutical industry, as it is difficult to ascertain whether the failure of a drug is due to its inability to reach the target or whether the target is not influencing cancer

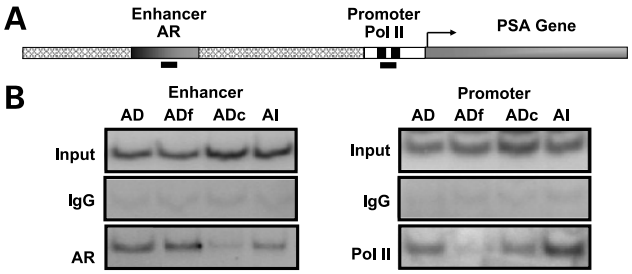

Figure 4. Chromatin immunoprecipitation of androgen receptor and polymerase II (*Pol II*) in flutamide-treated tumors. **A,** schematic of the PSA regulatory region and location of primer sets surrounding androgen receptor sites in the enhancer and promoter. Sequence details on the primers can be found in ref. 14. **B,** binding of androgen receptor to the enhancer. Androgen receptor or IgG antibodies were used to immunoprecipitate sheared chromatin from formaldehyde cross-linked tumors isolated from mice bearing LAPC9 androgen-dependent, flutamide-treated androgen-dependent tumors, tumors from mice castrated 10 d before harvest, and tumors stably grown in castrated animals. The DNA in the precipitates was amplified using the primers to the PSA enhancer, which amplifies the region containing multiple androgen receptor – binding sites. Input samples represent 2% of the starting sample before chromatin immunoprecipitation. **C,** polymerase II binding to the proximal promoter was measured by chromatin immunoprecipitation using a polymerase II CTD antibody (Covance, Berkeley, CA). IgG is a mock immunoprecipitation to assess background levels of precipitation.

growth. A second application of imaging is to identify periods when a drug is displaying maximal efficacy to perform invasive analyses to understand the mechanism of inhibition.

We employed the antiandrogen flutamide to test the ability of our TSTA molecular imaging system to measure the effect of a known small-molecule pharmaceutical on a specific signaling pathway in a live animal and to contrast the effects with our previous study on another standard treatment, androgen deprivation. We used adenovirus to deliver the TSTA imaging system because the xenografts used here do not grow as lines in cell culture and hence cannot be stably transformed with an imaging vector.

Our study led to the following conclusions: Flutamide significantly inhibits androgen receptor function in androgen-dependent prostate cancer xenografts, although the magnitude of the inhibition seems less than that observed by androgen withdrawal (~3-fold for flutamide and 10-fold for androgen withdrawal) reported in our previous study. The imaging signal and trends accurately recapitulate the effect of the flutamide on PSA levels, a clinical benchmark of prostate cancer. Yet, imaging with AdTSTA was more sensitive than serum PSA levels and reliably identified flutamide-mediated inhibition at earlier time points. Despite our previous observation that androgen receptor is fully active in androgen-independent cancer (14), androgen receptor signaling is highly resistant to flutamide inhibition.

With imaging, we were able to identify time points when the effect of flutamide was immediately evident and then harvest tumors to evaluate the molecular effects using immunoblotting and chromatin immunoprecipitation. From these analyses, we made the following observations. In contrast to the effects of androgen withdrawal by castration, flutamide did not inhibit androgen receptor binding to the PSA regulatory region but did inhibit polymerase II binding to the promoter. This effect occurred despite the observation that levels of androgen receptor

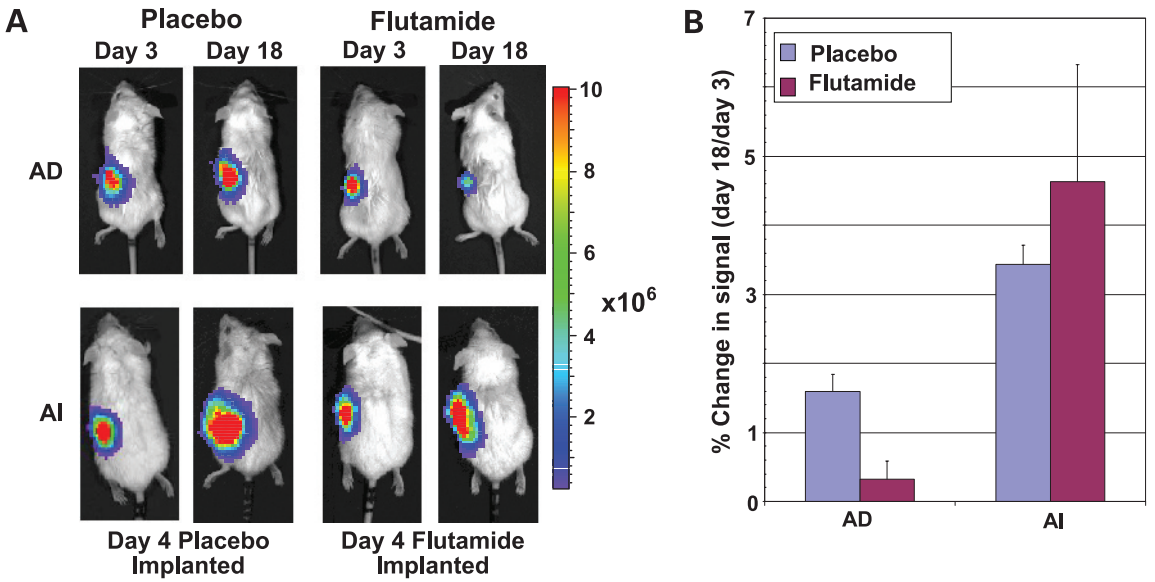

Figure 5. LAPC9 androgen-independent tumors are resistant to flutamide. AdTSTA were injected i.t. into intact or castrated male mice bearing LAPC9 xenografts. **A,** typical effects. On day 3, a baseline image was acquired and flutamide or placebo pellets were implanted. The effect of treatment at day 18 is shown. We have not detected any flutamide effect in the LAPC9 androgen-independent tumor model. **B,** cohorts of androgen-dependent ($n = 7$) and androgen-independent ($n = 6$) animals were studied. *Columns,* percent change in signal versus day 3 in placebo- and flutamide-treated animals bearing androgen-dependent and androgen-independent tumors.

and several of its coactivators are elevated in flutamide-treated tumors. Therefore, we conclude that antiandrogens and androgen withdrawal have distinct mechanisms of inhibition within the context of a tumor.

One of the key differences between the effects of androgen withdrawal and flutamide is the level of androgen receptor. In castrated animals, the tumor levels of androgen receptor decrease at the earliest time point, where the imaging revealed the inhibition. In contrast, flutamide increases the levels of androgen receptor at points where the inhibition is initially observed. The data are reminiscent of the stabilizing effect of dihydrotestosterone on androgen receptor (30, 31).

Our previous data along with cell culture studies show that castration or androgen deprivation causes the remaining androgen receptor to localize largely in the cytoplasm. Flutamide and Casodex, however, promote nuclear localization (39–41), which may in turn enhance androgen receptor stability and DNA binding. Consistent with this notion was our observation that androgen receptor binding to the PSA enhancer clearly decreases in tumors of castrate mice but remains bound in flutamide. Androgen receptor binding also occurs in LNCaP cells in the presence of another antiandrogen bicalutamide (42).

Polymerase II seems to bind the PSA promoter in castrate animals, although it is generally not found within the coding region. In contrast, we find little polymerase II bound to the promoter in the presence of flutamide. This observation in the tumor is consistent with cell culture studies showing that Casodex may actively repress the *PSA* gene by permitting androgen receptor to interact with corepressors (32, 43, 44). In addition, flutamide decreases the association of androgen receptor with various coactivators including TIF2, which in turn affects androgen receptor–mediated transcriptional activity (43, 45). Therefore, it is more likely that flutamide inhibits androgen receptor–mediated transcription through rearranging the cofactor environment on a promoter than affecting nuclear localization and DNA binding.

References

1. Feldman BJ, Feldman D. The development of androgen-independent prostate cancer. Nat Rev Cancer 2001;1:34–45.

2. Gelmann EP. Molecular biology of the androgen receptor. J Clin Oncol 2002;20:3001–15.

3. Cronauer MV, Schulz WA, Burchardt T, et al. The androgen receptor in hormone-refractory prostate cancer: relevance of different mechanisms of androgen receptor signaling [review]. Int J Oncol 2003;23:1095–102.

4. Schulz WA, Burchardt M, Cronauer MV. Molecular biology of prostate cancer. Mol Hum Reprod 2003;9:437–48.

5. Chen CD, Welsbie DS, Tran C, et al. Molecular determinants of resistance to antiandrogen therapy. Nat Med 2004;10:33–9.

6. Mellinghoff IK, Tran C, Sawyers CL. Growth inhibitory effects of the dual ErbB1/ErbB2 tyrosine kinase inhibitor PKI-166 on human prostate cancer xenografts. Cancer Res 2002;62:5254–9.

7. Mellinghoff IK, Vivanco I, Kwon A, Tran C, Wongvipat J, Sawyers CL. HER2/*neu* kinase-dependent modulation of androgen receptor function through effects on DNA binding and stability. Cancer Cell 2004;6:517–27.

8. Mohler JL, Gregory CW, Ford OH III, et al. The androgen axis in recurrent prostate cancer. Clin Cancer Res 2004;10:440–8.

9. Weber MJ, Gioeli D. Ras signaling in prostate cancer progression. J Cell Biochem 2004;91:13–25.

10. Culig Z. Androgen receptor cross-talk with cell signalling pathways. Growth Factors 2004;22:179–84.

11. Edwards J, Bartlett JM. The androgen receptor and signal-transduction pathways in hormone-refractory prostate cancer. Part 2. Androgen-receptor cofactors and bypass pathways. BJU Int 2005;95:1327–35.

12. Asatiani E, Gelmann EP. Targeted therapies for prostate cancer. Expert Opin Ther Targets 2005;9:283–98.

13. Zhang L, Adams JY, Billick E, et al. Molecular engineering of a two-step transcription amplification (TSTA) system for transgene delivery in prostate cancer. Mol Ther 2002;5:223–32.

14. Zhang L, Johnson M, Le KH, et al. Interrogating androgen receptor function in recurrent prostate cancer. Cancer Res 2003;63:4552–60.

15. Sato M, Johnson M, Zhang L, et al. Optimization of adenoviral vectors to direct highly amplified prostate-specific expression for imaging and gene therapy. Mol Ther 2003;8:726–37.

16. Iyer M, Wu L, Carey M, Wang Y, Smallwood A, Gambhir SS. Two-step transcriptional amplification as a method for imaging reporter gene expression using weak promoters. Proc Natl Acad Sci U S A 2001;98:14595–600.

17. Craft N, Shostak Y, Carey M, Sawyers CL. A mechanism for hormone-independent prostate cancer through modulation of androgen receptor signaling by the HER-2/neu tyrosine kinase. Nat Med 1999;5:280–5.

18. Singh SM, Gauthier S, Labrie F. Androgen receptor antagonists (antiandrogens): structure-activity relationships. Curr Med Chem 2000;7:211–47.

19. Luo S, Martel C, Chen C, et al. Daily dosing with flutamide or Casodex exerts maximal antiandrogenic activity. Urology 1997;50:913–9.

20. Massoud TF, Gambhir SS. Molecular imaging in living subjects: seeing fundamental biological processes in a new light. Genes Dev 2003;17:545–80.

21. Choy G, Choyke P, Libutti SK. Current advances in molecular imaging: noninvasive *in vivo* bioluminescent and fluorescent optical imaging in cancer research. Mol Imaging 2003;2:303–12.

22. Ray S, Paulmurugan R, Hildebrandt I, et al. Novel bidirectional vector strategy for amplification of therapeutic and reporter gene expression. Hum Gene Ther 2004;15:681–90.

23. Bhaumik S, Lewis XZ, Gambhir SS. Optical imaging of *Renilla* luciferase, synthetic *Renilla* luciferase, and firefly luciferase reporter gene expression in living mice. J Biomed Opt 2004;9:578–86.

24. Herschman HR. Molecular imaging: looking at problems, seeing solutions. Science 2003;302:605–8.

25. Sadowski I, Ma J, Triezenberg S, Ptashne M. GAL4-VP16 is an unusually potent transcriptional activator. Nature 1988;335:563–4.

26. Emami KH, Carey M. A synergistic increase in potency of a multimerized VP16 transcriptional activation domain. EMBO J 1992;11:5005–12.

27. Wu L, Matherly J, Smallwood A, et al. Chimeric PSA enhancers exhibit augmented activity in prostate cancer gene therapy vectors. Gene Ther 2001;8:1416–26.

28. Iyer M, Salazar FB, Lewis X, et al. Noninvasive imaging of enhanced prostate-specific gene expression using a two-step transcriptional amplification-based lentivirus vector. Mol Ther 2004;10:545–52.

29. Sato M, Johnson M, Zhang L, Gambhir SS, Carey M, Wu L. Functionality of androgen receptor-based gene expression imaging in hormone refractory prostate cancer. Clin Cancer Res 2005;11:3743–9.

30. Zhou ZX, Lane MV, Kemppainen JA, French FS, Wilson EM. Specificity of ligand-dependent androgen receptor stabilization: receptor domain interactions influence ligand dissociation and receptor stability. Mol Endocrinol 1995;9:208–18.

31. Kemppainen JA, Wilson EM. Agonist and antagonist activities of hydroxyflutamide and Casodex relate to androgen receptor stabilization. Urology 1996;48:157–63.

32. Shang Y, Myers M, Brown M. Formation of the androgen receptor transcription complex. Mol Cell 2002;9:601–10.

33. Comuzzi B, Lambrinidis L, Rogatsch H, et al. The transcriptional co-activator cAMP response element-binding protein-binding protein is expressed in prostate cancer and enhances androgen- and anti-androgen-induced androgen receptor function. Am J Pathol 2003;162:233–41.

34. Kim J, Jia L, Tilley WD, Coetzee GA. Dynamic methylation of histone H3 at lysine 4 in transcriptional regulation by the androgen receptor. Nucleic Acids Res 2003;31:6741–7.

35. Nelson WG, De Marzo AM, Isaacs WB. Prostate cancer. N Engl J Med 2003;349:366–81.

36. Veldscholte J, Ris-Stalpers C, Kuiper GG, et al. A mutation in the ligand binding domain of the androgen receptor of human LNCaP cells affects steroid binding characteristics and response to anti-androgens. Biochem Biophys Res Commun 1990;173:534–40.

37. Matias PM, Carrondo MA, Coelho R, et al. Structural basis for the glucocorticoid response in a mutant human androgen receptor (AR(ccr)) derived from an androgen-independent prostate cancer. J Med Chem 2002;45:1439–46.

38. Hara T, Miyazaki J, Araki H, et al. Novel mutations of androgen receptor: a possible mechanism of bicalutamide withdrawal syndrome. Cancer Res 2003;63:149–53.

39. Karvonen U, Janne OA, Palvimo JJ. Pure antiandrogens disrupt the recruitment of coactivator GRIP1 to colocalize with androgen receptor in nuclei. FEBS Lett 2002;523:43–7.

40. Tomura A, Goto K, Morinaga H, et al. The subnuclear three-dimensional image analysis of androgen receptor fused to green fluorescence protein. J Biol Chem 2001;276:28395–401.

41. Tyagi RK, Lavrovsky Y, Ahn SC, Song CS, Chatterjee B, Roy AK. Dynamics of intracellular movement and nucleocytoplasmic recycling of the ligand-activated androgen receptor in living cells. Mol Endocrinol 2000;14:1162–74.

42. Masiello D, Cheng S, Bubley GJ, Lu ML, Balk SP. Bicalutamide functions as an androgen receptor antagonist by assembly of a transcriptionally inactive receptor. J Biol Chem 2002;277:26321–6.

43. Berrevoets CA, Umar A, Trapman J, Brinkmann AO. Differential modulation of androgen receptor transcriptional activity by the nuclear receptor co-repressor (N-CoR). Biochem J 2004;379:731–8.

44. Kang Z, Janne OA, Palvimo JJ. Coregulator recruitment and histone modifications in transcriptional regulation by the androgen receptor. Mol Endocrinol 2004;18:2633–48.

45. Matsuda T, Junicho A, Yamamoto T, et al. Cross-talk between signal transducer and activator of transcription 3 and androgen receptor signaling in prostate carcinoma cells. Biochem Biophys Res Commun 2001;283:179–87.

Molecular Cancer Therapeutics

Imaging androgen receptor function during flutamide treatment in the LAPC9 xenograft model

Romyla Ilagan, Liquin Joann Zhang, Jill Pottratz, et al.

Mol Cancer Ther 2005;4:1662-1669.